

This content has been downloaded from IOPscience. Please scroll down to see the full text.

Download details:

IP Address: 18.117.107.234

This content was downloaded on 12/05/2024 at 13:46

Please note that [terms and conditions apply](#).

You may also like:

[Analysis of resonant planar dissipative network antennas for rf inductively coupled plasma sources](#)

Ph Guittienne, A A Howling and Ch Hollenstein

[Industrial plasmas in academia](#)

Ch Hollenstein, AA Howling, Ph Guittienne et al.

[A FEM Based on the Parametric Variational Principle for the Cable-network Antenna's Form-finding Design](#)

Tao Liu, Hao Li, Guoan Tang et al.

[Complex image method for RF antenna-plasma inductive coupling calculation in planar geometry. Part II: measurements on a resonant network](#)

Ph Guittienne, R Jacquier, A A Howling et al.

[Resonant RF network antennas for large-area and large-volume inductively coupled plasma sources](#)

Ch Hollenstein, Ph Guittienne and A A Howling

Resonant Network Antennas for Radio-Frequency Plasma Sources

Theory, technology and applications

Online at: <https://doi.org/10.1088/978-0-7503-5296-3>

IOP Series in Plasma Physics

Series Editor

Richard Dendy

Culham Centre for Fusion Energy and the University of Warwick, UK

About the series

The IOP Plasma Physics ebook series aims at comprehensive coverage of the physics and applications of natural and laboratory plasmas, across all temperature regimes. Books in the series range from graduate and upper-level undergraduate textbooks, research monographs and reviews.

The conceptual areas of plasma physics addressed in the series include:

- Equilibrium, stability, and control.
- Waves: fundamental properties, emission, and absorption.
- Nonlinear phenomena and turbulence.
- Transport theory and phenomenology.
- Laser–plasma interactions.
- Non-thermal and suprathermal particle populations.
- Beams and non-neutral plasmas.
- High energy density physics.
- Plasma–solid interactions, dusty, complex, and non-ideal plasmas.
- Diagnostic measurements and techniques for data analysis.

The fields of application include:

- Nuclear fusion through magnetic and inertial confinement.
- Solar–terrestrial and astrophysical plasma environments and phenomena.
- Advanced radiation sources.
- Materials processing and functionalisation.
- Propulsion, combustion, and bulk materials management.
- Interaction of plasma with living matter and liquids.
- Biological, medical, and environmental systems.
- Low-temperature plasmas, glow discharges, and vacuum arcs.
- Plasma chemistry and reaction mechanisms.
- Plasma production by novel means.

A full list of titles published in this series can be found here: <https://iopscience.iop.org/bookListInfo/iop-plasma-physics-series>.

Resonant Network Antennas for Radio-Frequency Plasma Sources

Theory, technology and applications

Philippe Guittienne

Alan Howling

Ivo Furno

*Ecole Polytechnique Fédérale de Lausanne (EPFL), Swiss Plasma Center (SPC),
CH-1015 Lausanne, Switzerland*

IOP Publishing, Bristol, UK

© IOP Publishing Ltd 2024

All rights reserved. No part of this publication may be reproduced, stored in a retrieval system or transmitted in any form or by any means, electronic, mechanical, photocopying, recording or otherwise, without the prior permission of the publisher, or as expressly permitted by law or under terms agreed with the appropriate rights organization. Multiple copying is permitted in accordance with the terms of licences issued by the Copyright Licensing Agency, the Copyright Clearance Centre and other reproduction rights organizations.

Permission to make use of IOP Publishing content other than as set out above may be sought at permissions@iopublishing.org.

Philippe Guittienne, Alan Howling and Ivo Furno have asserted their right to be identified as the authors of this work in accordance with sections 77 and 78 of the Copyright, Designs and Patents Act 1988.

ISBN 978-0-7503-5296-3 (ebook)
ISBN 978-0-7503-5294-9 (print)
ISBN 978-0-7503-5297-0 (myPrint)
ISBN 978-0-7503-5295-6 (mobi)

DOI 10.1088/978-0-7503-5296-3

Version: 20240201

IOP ebooks

British Library Cataloguing-in-Publication Data: A catalogue record for this book is available from the British Library.

Published by IOP Publishing, wholly owned by The Institute of Physics, London

IOP Publishing, No.2 The Distillery, Glassfields, Avon Street, Bristol, BS2 0GR, UK

US Office: IOP Publishing, Inc., 190 North Independence Mall West, Suite 601, Philadelphia, PA 19106, USA

Contents

Preface	xiv
Acknowledgements	xv
Author biographies	xvi
Glossary	xix
1 Introduction	1-1
1.1 Resonant network antennas...	1-2
1.2 ...for radio-frequency plasma sources	1-4
1.2.1 Birdcage antenna helicon source	1-5
1.2.2 Ladder antenna inductive source	1-6
1.3 Evolution of the antenna design	1-6
1.4 Why use resonant network antennas?	1-8
1.5 Outline of the book	1-9
References	1-11
Part I Resonant network antennas without plasma	
2 Introduction to resonant circuits	2-1
2.1 Definitions and conventions	2-1
2.1.1 Angular frequency and wavenumber	2-1
2.1.2 Loop self inductance	2-2
2.2 Parallel resonant circuits	2-3
2.2.1 The lossless LC parallel circuit	2-3
2.2.2 The lossy LC parallel circuit	2-5
2.3 From lumped element inductor to transmission line	2-10
References	2-13
3 Normal modes and dissipative networks	3-1
3.1 Experimental set-up of the ladder antenna	3-1
3.2 Introduction to normal modes	3-5
3.3 General solution for the network currents	3-5
3.3.1 Characteristic equation on lossless networks	3-7
3.4 Normal mode solution for open networks	3-8
3.4.1 Normal mode frequencies on open networks	3-8

3.4.2	Normal mode currents on open networks	3-9
3.4.3	Normal mode voltages on open networks	3-10
3.4.4	Comparison with measurements on the ladder antenna	3-11
3.5	Dissipative networks: Helyssen plasma sources	3-15
3.5.1	Currents in a dissipative antenna with arbitrary RF connections	3-15
3.5.2	The leg currents in the three parts of the dissipative antenna	3-17
3.5.3	Driven resonance currents in the limit of weak dissipation	3-19
3.5.4	Input impedance of a dissipative antenna	3-20
3.5.5	Resonance frequencies of dissipative antennas	3-21
3.5.6	Parallel resonant equivalent circuit for dissipative antennas	3-23
3.5.7	Optimization of the input impedance for antenna design	3-26
3.6	Application: frequency resolution of MRI antennas	3-27
3.7	Chapter summary	3-28
	References	3-29
4	Partial inductance and the matrix model	4-1
4.1	A brief history of inductance: loop and partial	4-1
4.2	Can the self inductance of a wire be measured?	4-2
4.2.1	Measurement of a coil's self inductance	4-3
4.2.2	Measurement of a straight wire's self inductance	4-4
4.3	Definition of partial inductance	4-4
4.3.1	Step 1: introduce the magnetic vector potential \mathbf{A}	4-5
4.3.2	Step 2: convert to a contour integral around the loop	4-5
4.3.3	Step 3: decomposition of the contour	4-6
4.3.4	Step 4: magnetic vector potential due to a line current	4-6
4.3.5	Step 5: partial contributions to the magnetic vector potential	4-8
4.3.6	Step 6: self partial inductance and mutual partial inductance	4-9
4.4	Calculation of the partial inductance of wires	4-12
4.4.1	Partial inductance by integration of the magnetic vector potential	4-13
4.4.2	Partial inductance by integration of the magnetic flux density	4-15
4.5	Relevant special cases of partial inductance	4-17
4.5.1	Parallel wires with anti-parallel currents	4-17
4.5.2	Mutual partial inductance of offset parallel wires	4-19
4.6	Antenna equivalent circuit including mutual partial inductance	4-22
4.7	Mutual partial inductance matrix equations	4-22
4.7.1	Effect of a planar screen on the mutual partial inductance matrix	4-24

4.8	Experiment and theory for an antenna without plasma	4-27
4.8.1	Voltage distribution of the network modes	4-27
4.8.2	Matrix model of the input impedance without plasma	4-27
4.8.3	Matrix model for the mode frequencies without plasma	4-28
4.9	Conclusions for part I	4-30
	References	4-30

Part II Resonant network antennas in non-magnetized plasma

5	Introduction to inductively coupled plasma	5-1
5.1	RF plasma generalities	5-1
5.1.1	Why use plasma?	5-1
5.1.2	Why use radio frequency?	5-2
5.1.3	Why use low pressure?	5-3
5.2	RF plasma sources in non-magnetized plasma	5-4
5.2.1	Capacitively coupled RF reactors: the <i>E</i> -mode	5-4
5.2.2	Inductively coupled RF reactors: the <i>H</i> -mode	5-5
5.2.3	Large-scale RF reactors: the <i>EM</i> -mode	5-6
5.3	Skin depth in inductively coupled plasma	5-7
5.3.1	Collisional skin depth	5-7
5.3.2	Collisionless skin depth	5-8
5.4	Transformer model for inductively coupled plasma	5-9
5.4.1	Loop inductances for a solenoid ICP reactor	5-9
5.4.2	Transformer model for a solenoid ICP reactor	5-10
5.4.3	Comparison between transformer and image models for ICP	5-11
5.5	Prohibitively high voltages in large area ICP	5-13
5.6	Chapter summary for the introduction to ICP	5-15
	References	5-15
6	Inductive coupling using plane plasma sources	6-1
6.1	Introduction to planar ICP sources	6-1
6.2	Experimental set-up for an ICP ladder resonant antenna	6-4
6.2.1	Plasma diagnostics	6-6
6.3	Plasma performance of an ICP ladder resonant antenna	6-7
6.3.1	Transition from <i>E</i> -mode to <i>H</i> -mode	6-9
6.3.2	Plasma uniformity for spiral coil and ladder resonant antenna	6-11
6.3.3	Diffusion profiles close to reactor sidewalls	6-12

6.4	Induced currents in the plasma: the complex image method	6-13
6.4.1	The impedance loading spectrum when inductively coupled to plasma	6-13
6.4.2	Inductive coupling of straight wires to plane plasma—the complex image method	6-16
6.4.3	Complex image model for the loading spectrum	6-18
6.5	Application: RF biasing for plasma deposition	6-24
6.6	Chapter summary for inductive, plane plasma sources	6-25
	References	6-26
7	Electromagnetic coupling to plasma in large antennas	7-1
7.1	Electromagnetic effects in large area antennas	7-3
7.1.1	Existing models of ICP sources	7-4
7.1.2	Comparison of large area ICP sources	7-4
7.2	Experimental set-up for large area antennas	7-5
7.2.1	RF electrical configurations—antenna grounded or DC floating	7-6
7.2.2	Diagnostics and plasma parameters	7-8
7.3	Single conductor lossy transmission line	7-9
7.4	Multi-conductor transmission line (MTL)	7-10
7.5	Experiment and MTL model for the vacuum case	7-11
7.5.1	Measurements in a vacuum with a grounded antenna	7-12
7.5.2	Measurements in a vacuum with a DC floating antenna	7-14
7.6	Experiment and MTL model with plasma loading	7-16
7.6.1	Partial inductance matrix for the MTL plasma-coupled antenna	7-16
7.6.2	Capacitance matrix for the MTL plasma-coupled antenna	7-18
7.6.3	Measurements in plasma with a grounded antenna	7-19
7.6.4	Measurements in plasma with a DC-floating antenna	7-21
7.6.5	Plasma uniformity	7-23
7.6.6	Summary for large area RF plasma sources	7-24
7.7	Applications of EM-coupled antennas	7-25
7.7.1	Application: deposition of barrier coatings on polymers for the packaging industry	7-25
7.7.2	Application: high-frequency inductive antenna probe to measure the plasma complex conductivity	7-27
7.8	Chapter summary for <i>EM</i> -coupled antennas	7-32
	References	7-32

8	Cylindrical wave functions in birdcage antennas	8-1
8.1	A general wavefield solution for birdcage antennas	8-2
8.1.1	Shell surface current density	8-6
8.2	Vacuum wavefields for a $m = 1$ shell current inside a PEC screen	8-8
8.2.1	Low frequency limit for $m = 1$ shell current inside a PEC screen	8-16
8.2.2	Dynamics of the vacuum wavefields in the low-frequency limit inside an $m = 1$ shell current	8-18
8.3	Vacuum wavefields of a birdcage within a PEC screen	8-20
8.3.1	Surface current density due to a wire current on the shell radius	8-20
8.3.2	Vacuum wavefields for a wire current inside a PEC screen	8-21
8.3.3	Vacuum wavefields for a birdcage within a screen	8-22
8.4	Plasma coupling by a shell current within a PEC screen	8-24
8.4.1	Inductive power transfer in a birdcage antenna	8-29
8.5	Image method for birdcage antennas	8-31
8.5.1	Apollonius image current for a wire in a PEC cylindrical screen	8-31
8.5.2	Complex image method for birdcage plasma sources	8-35
8.6	Chapter summary for wavefields in birdcage antennas	8-36
	References	8-36
9	Inductive plasma generated by a birdcage antenna	9-1
9.1	Birdcage construction	9-1
9.2	Normal modes on closed networks	9-2
9.2.1	Normal mode frequencies on closed networks	9-3
9.2.2	Mode structure in closed birdcage antennas	9-5
9.2.3	Inductive magnetic field measurement for mode $m = 1$	9-6
9.2.4	RF power connection configuration	9-8
9.2.5	Voltage and current measurements on birdcage antennas	9-9
9.2.6	Power measurement in a resonant network antenna	9-10
9.3	Applications of birdcage inductive antennas	9-12
9.3.1	Application: plasma treatment of powder in a fluidized bed	9-12
9.3.2	Application: plasma deposition in a large volume birdcage	9-14
9.4	Chapter summary for inductive birdcages	9-18
	References	9-18

Part III Resonant network antennas in magnetized plasma

10 Whistler waves in an infinite uniform magnetized plasma	10-1
10.1 Introduction and classification of plasma waves	10-2
10.1.1 Waves considered here: electromagnetic electron waves in unbounded, magnetized plasma	10-3
10.1.2 Waves not considered here	10-3
10.2 Revision of polarization in magnetized plasma	10-4
10.2.1 Linear polarization	10-4
10.2.2 Circular polarization, right and left	10-4
10.3 Conductivity and permittivity tensors in uniform magnetoplasma	10-8
10.3.1 Solution using electron fluid velocity components	10-8
10.4 Plane wave dispersion relations in collisionless magnetoplasma	10-11
10.5 Solution of the principal wave dispersion relations	10-12
10.6 Wave number parallel to the magnetic field	10-13
10.6.1 Langmuir ‘wave’	10-14
10.6.2 R-wave	10-14
10.6.3 L-wave	10-17
10.6.4 Wave number perpendicular to the magnetic field	10-18
10.7 Electromagnetic electron wave cut-offs and resonances	10-18
10.8 Unbounded collisionless motion at the electron cyclotron resonance: explicit time solution	10-22
10.9 Bounded collisional motion: explicit time solution	10-26
10.10 Whistler propagation, or evanescence and reflection in collisionless plasma	10-30
10.11 Two approximate methods for an arbitrary angle of plane waves in magnetized plasma	10-35
10.11.1 Neglecting the vacuum displacement current	10-36
10.11.2 Tensor approximation of the plane wave dispersion relation	10-37
10.11.3 Curl factorization approximation of the plane wave dispersion relation	10-39
10.12 Chapter summary for whistler waves in uniform, magnetized plasma	10-41
References	10-42
11 Helicon modes in a magnetized plasma column	11-1
11.1 Introduction to the helicon mode equations	11-2
11.1.1 The constitutive relations for the magnetized plasma column	11-4

11.1.2	The equations to be solved for various simplifying assumptions	11-4
11.1.3	Uniform plasma density and collisionality, but no vacuum displacement current	11-5
11.1.4	Radially non-uniform plasma density and collisionality, but no vacuum displacement current	11-8
11.1.5	Radially non-uniform plasma density, collisionality, and vacuum displacement current	11-11
11.1.6	Helicon approximation equations	11-12
11.1.7	Boundary conditions and mode quantization	11-13
11.2	Normal mode solutions for uniform plasma density	11-15
11.2.1	PEC at the plasma boundary, helicon approximation	11-15
11.2.2	PEC at the plasma boundary, collisionless {H,T-G} model	11-16
11.2.3	PEC at the plasma boundary, collisional {H,T-G} model	11-22
11.2.4	Vacuum plasma boundary, collisionless {H,T-G} model	11-26
11.2.5	Vacuum plasma boundary, collisional {H,T-G} model	11-27
11.2.6	Intermediate conclusions from the uniform density models	11-33
11.3	Normal mode solutions for radially non-uniform plasma	11-34
11.3.1	Collisional {H,T-G} model, non-uniform density	11-34
11.4	Chapter summary for helicon modes in a magnetized plasma	11-39
	References	11-39
12	Wave-sustained plasma	12-1
12.1	Bounded helicon discharge	12-2
12.2	Unbounded helicon discharges: the RAID experiment	12-5
12.2.1	Plasma characterization	12-7
12.2.2	Wave propagation	12-11
12.2.3	Main axial wavelength analysis	12-16
12.2.4	The R plane wave	12-18
12.2.5	Radially non-uniform density profile	12-18
12.2.6	Numerical simulation	12-19
12.2.7	Multimodal excitation	12-21
12.2.8	Impedance measurements, antenna coupling	12-24
12.3	Planar helicon plasma source	12-26
12.4	Applications of birdcage helicon antennas	12-34
12.4.1	Application: helicon plasma thruster using a birdcage antenna	12-34
12.4.2	Application: negative ion sources using birdcage antennas	12-34
12.5	Chapter summary for wave heated discharges	12-36
	References	12-36

Part IV Technology, future developments, and appendices

13	Technology of resonant network antennas	13-1
13.1	Impedance matching of resonant network antennas	13-1
13.1.1	Two element matching	13-2
13.1.2	T matching	13-3
13.2	Capacitor assemblies for high RF power antennas	13-10
13.2.1	Series and parallel assemblies	13-11
13.3	Dimensioning the RF system	13-12
13.3.1	The coaxial line	13-13
13.3.2	Impedance matching at the cable input	13-14
13.3.3	Potentials and currents	13-15
13.3.4	Study #1: resonant networks versus solenoid ICPs	13-17
13.3.5	Study #2: choosing a coaxial cable	13-21
13.3.6	Study #3: choosing the number of antenna legs	13-23
13.3.7	Study #4: choosing the antenna mode number	13-25
13.4	Antenna mechanical construction	13-28
13.4.1	Antennas operating in an atmospheric pressure environment	13-28
13.4.2	Antennas operating in a low pressure environment	13-31
13.5	High Q design	13-40
13.6	Chapter summary for the technology of resonant network antennas	13-46
	References	13-47
14	Future developments and applications	14-1
14.1	Hybrid design	14-1
14.2	Two-dimensional resonant network antennas	14-6
14.2.1	Matrix formalism	14-8
14.2.2	Verifying the boundaries	14-9
14.2.3	Modes in 2D networks	14-11
14.3	Phased antennas	14-15
14.4	Toroidal plasma generated by a birdcage antenna	14-19
14.5	Multiple birdcage antennas along a plasma column	14-20
14.6	Matchless antennas	14-21
14.7	Conclusions	14-21
	References	14-22

Appendix A: Expansions near resonance for the dissipative antenna	A-1
Appendix B: Impedance matrix calculations	B-1
Appendix C: Electron–molecule energy transfer fraction	C-1
Appendix D: Maxwell’s equations, plasma permittivity, and skin depth	D-1
Appendix E: Theory of the complex image method	E-1
Appendix F: Solution of the MTL equations for the EMCP antenna source	F-1
Appendix G: Maxwell’s potential coefficient matrix and the partial image method	G-1
Appendix H: Impedance of a hybrid antenna with parasitic capacitance	H-1
Appendix I: Cylindrical wave function constants	I-1
Appendix J: Helicon mode derivations and methods	J-1
Appendix K: Link to programs	K-1

Preface

Radio frequency plasmas provide the underlying technology for many of today's critical semiconductor industries. The demand for larger and more uniform plasma sources is reaching the limits of conventional capacitive and inductive RF plasma reactors, due to standing wave effects and the asymptotic impedance of large-area reactors. The inherent properties of resonant network antennas can overcome these limitations because of their spatially distributed internal resonances and real input impedance.

This book aims to show that resonant network antennas are versatile, alternative sources for inductively coupled and wave-driven plasma. The theory has developed alongside the technology (see also <https://www.helyssen.com>) to the extent that it is timely to document the progress in an accessible way, to aid antenna design for future RF plasma applications.

To maximize the usefulness of this book for the physicist, engineer, and student, we have taken care to provide all the necessary details for the reader. In particular:

- Equations are derived in full with all intermediate steps.
- Unfamiliar techniques, such as partial inductance calculations, the complex image method, and partial image theory are developed step-by-step from elementary principles by means of explanatory figures.
- The most useful and recurring antenna calculations are provided using a link to programs which reproduce the tensor solutions and many of the book's figures in appendix K.
- Basic concepts in plasma physics are explained, occasionally using a novel approach.

We assume an undergraduate science level familiar with complex numbers, complex impedance, and Maxwell's equations. The chapters and appendixes are cross-referenced throughout the book, but for the most part, the chapters can be read independently of each other. MKS SI units are used throughout. We use 'antennas' for the plural of 'antenna', with apologies to Latin scholars.

The readers will be grateful to Alex Howling, our illustrator, for bringing a touch of comic relief to each chapter.

Dr Philippe Guittienne
Dr Alan Howling
Professor Ivo Furno
Lausanne, Switzerland,
26 October 2023

Acknowledgements

We are indebted to Rémy Jacquier, our master engineer, for his contribution to the construction of, and experiments on, the various plasma reactors. We are grateful to the former group leader and co-founder (with Alan Howling and Pierre-Jean Paris in 1989) of the Industrial Plasma Applications Group, Dr Christoph Hollenstein (now retired), for his foresight and generosity in supporting the fledgling Helyssen plasma sources at the CRPP. Our thanks also go to: Helyssen Sàrl director Alain Dannaoui, Gennady Plyushchev, Riccardo Agnello, Fabio Avino, Basile Pouradier Duteil, Cédric Vivien, Claudio Marini, Pierre Demolon, Renat Karimov, Simon Vincent, Marcelo Baquero, Christine Stollberg, Lyes Kadi, Christian Schlatter, Edith Grueter, Yves Martin, Stefano Alberti, Duccio Testa, Pierre Fayet, Sylvain Lecoultre, Antonio d'Angola, Alain Simonin, Stephane Béchu, Hamza Drissikamili, Zacharie Jehan, Arthur Wuhrmann, Benjamin Forster, Andrii Shytikov, the technical services and workshops, and the Swiss Plasma Center directorate, especially Professor Ambrogio Fasoli, for their continual support.

The authors and the Basic Plasma Physics and Applications Group of the Swiss Plasma Center, Ecole Polytechnique Fédérale de Lausanne, wish to thank the Innosuisse Swiss Innovation Agency (formerly the CTI Commission for Technology and Innovation) for their support. Part of this work has been carried out within the framework of the EUROfusion Consortium, via the Euratom Research and Training Programme (Grant Agreement No 101 052 200—EUROfusion) and funded by the Swiss State Secretariat for Education, Research and Innovation (SERI). Views and opinions expressed are however those of the author(s) only and do not necessarily reflect those of the European Union, the European Commission, or SERI. Neither the European Union nor the European Commission nor SERI can be held responsible for them.

Individual projects are acknowledged in full in the publications referenced throughout the book.

Author biographies

Philippe Guittienne



Dr Philippe Guittienne is currently a physicist at the Swiss Plasma Center (SPC) in the Basic Plasma Physics and Applications group under Professor Ivo Furno, and founder of the Helyssen Sàrl company in 2003. Following an engineering degree in physics (1997) and a doctorate (2002) in condensed matter physics at the EPFL on magnetization reversal in ferromagnetic nanostructures, he completely changed his field of interest to birdcages for helicon sources, inspired by the PhD on MRI of his future wife, Jacqueline.

On the basis of this intuition, he founded the Helyssen Sàrl start-up in 2003, and started a collaboration with Dr Christoph Hollenstein's group at SPC for the development of resonant antennas as plasma sources. This topic turned out to be a fruitful field of research, and during the years it became a central part of the Industrial Plasma Group (now included in Basic Plasma Physics and Applications), and is, indeed, the subject of this book.

Alan Arthur Howling



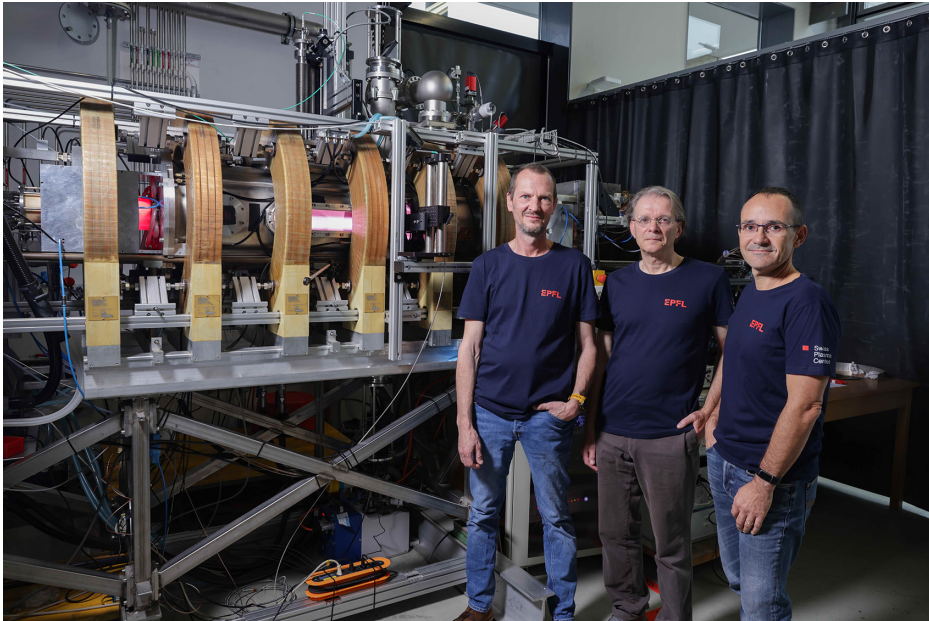
Dr Alan Arthur Howling is an Adjoint Scientifique/Senior Scientific Collaborator, co-founder of the group for industrial plasmas in 1989 with Dr Christoph Hollenstein. He is currently a researcher and lecturer in the Basic Plasma Physics and Applications group under Professor Ivo Furno at the Swiss Plasma Center, EPFL, Lausanne, Switzerland. A Gordon Warter Open Scholarship in 1978 to Pembroke College, Oxford University, led to a physics (Natural Sciences) degree in 1981, followed by an MSc and Gordon Francis

prize (1982) in the Science and Applications of Electric Plasmas at Wolfson College, Oxford University, and then a doctorate titled 'Fluctuations in the edge plasma of the TOSCA tokamak' (1985) at both Oxford and UKAEA Culham Laboratory, as it was then called. A postdoc on the TCA tokamak in the Centre de Recherches en Physique des Plasmas (CRPP), EPFL Lausanne, Switzerland from 1986 to 1989 was the springboard to RF industrial plasmas in 1989. Applied research topics included negative ion polymerization (silanions) and particle formation in silane RF plasmas; design of large-area RF capacitive plasma reactors for solar cells and flat panel displays, including showerhead uniformity, discharge equilibration, plasmoids, and electromagnetic analysis of symmetric and anti-symmetric modes; RF plasma deposition of amorphous and micro-crystalline silicon; RF plasma diagnostics and glass substrate charging; design of resonant ladder networks for RF plasmas, introducing partial inductance and complex image methods; high voltage design of satellite slip-rings; bio-plasma with Alexandra Waskow and the effect of humidity on dielectric barrier discharges; finally concentrating on writing this swan-song book before retirement on 26 October 2023.

Ivo Furno



Professor Ivo Furno is currently Adjunct Professor at the EPFL and leader of the Basic Plasma Physics and Applications (BPPA) group of the Swiss Plasma Center. He graduated in Nuclear Engineering from the Politecnico di Torino, Italy, in 1995 and then received his PhD from the EPFL with a thesis on ‘Fast transient transport phenomena measured by soft x-ray emission in TCV tokamak plasmas’. He continued with a postdoc at the Los Alamos National Laboratory, where he studied magnetic reconnection on the Reconnection Scaling Experiment (RSX), before re-joining the EPFL in 2006. His research is marked by the use of human-scale, dedicated plasma devices to investigate the fundamental physics of plasmas under conditions ranging from fusion plasmas to plasmas of relevance for solar physics and to non-equilibrium cold plasmas for industrial and biological applications. For his work on turbulence in magnetized plasmas, he was awarded the Fellowship of the American Physics Society. On the TCV tokamak, he contributed to the development of the first experiments on the so-called snowflake divertor, and, recently, he led the TCV team that obtained the first experimental demonstration of electron cyclotron microwave beam broadening by plasma turbulence. Since he took over the responsibility of the BPPA group, he has obtained numerous grants to develop industrial applications in collaboration with national academic institutions as well as with industrial partners. He developed the Resonant Antenna Ion Device (RAID) and launched its scientific program to study the physics of helicon waves and negative ion volume generation in helicon plasmas. As part of the new SPC activities beyond fusion, he started collaborating with CERN in the field of wakefield acceleration for the next-generation particle accelerator. The SPC is today an active member of the AWAKE Consortium. A new laboratory for societal, e.g. biological, applications of plasmas, such as plasma agriculture and plasma sterilization, was launched by Furno to expand the SPC infrastructure into atmospheric pressure plasmas for fundamental life science projects. It was Furno who originally proposed writing this book, titled *Resonant Network Antennas for Radio-Frequency Plasma Sources*.



The authors in front of the RAID device: Philippe Guittienne, Alan Howling, and Ivo Furno.

Glossary

Greek terms

α	attenuation constant per section
α_m	a Fourier coefficient
β	phase change per section (rad)
β_m	a Fourier coefficient
$\beta_{1,2}$	wavenumber for H, TG modes (m^{-1})
γ	propagation constant
Δf	FWHM bandwidth (Hz)
δ	Dirac delta function
$\delta\omega$	a small difference in angular frequency from the resonance frequency (rad s^{-1})
$\Delta\omega$	the FWHM half-power bandwidth in angular frequency (rad s^{-1})
ϵ_0	permittivity of free space (F m^{-1})
ϵ_p	relative permittivity of unmagnetized plasma (-)
$\bar{\epsilon}_p$	tensor relative permittivity of magnetized plasma (-)
ξ_m	a Fourier coefficient
η	power transfer efficiency
θ	angle of propagation with respect to the magnetic field
λ	wavelength (m)
μ_0	permeability of free space (H m^{-1})
ν	effective collision frequency (s^{-1})
ν_m	electron-neutral collision frequency (s^{-1})
ξ_m	a Fourier coefficient
ρ	free charge density (C m^{-3})
ρ_{dc}	DC electrical resistivity ($\Omega \text{ m}$)
ρ_p	plasma complex electrical resistivity ($\Omega \text{ m}$)
σ_{dc}	DC electrical conductivity (S m^{-1})
σ_{en}	electron-neutral collision cross-section (m^2)
σ_p	complex electrical conductivity of unmagnetized plasma (S m^{-1})
$\bar{\sigma}_p$	tensor electrical conductivity of magnetized plasma (S m^{-1})
τ	RF period $= 2\pi/\omega$ (s)
Φ	total magnetic flux linkage (Wb)
ϕ	azimuthal angle in cylindrical coordinates (r, ϕ, z)
ω	angular (RF) frequency (rad s^{-1})
$\hat{\omega}$	$(\omega + j\nu)$
ω_0	resonance angular frequency for an ideal (lossless) circuit (rad s^{-1})
ω'_0	resonance angular frequency for a real (lossy) circuit (rad s^{-1})
ω_m	angular frequency of the mth normal mode (rad s^{-1})
ω_{ci}	ion cyclotron angular frequency (rad s^{-1})
ω_{ce}	electron cyclotron angular frequency (rad s^{-1})

Symbols, abbreviations, and subscripts

$\bar{\mathbf{I}}$	$N \times N$ identity matrix
1D, 2D	one-dimensional, two-dimensional
\mathbf{A}	vector magnetic potential (Wb m^{-1})
\mathbf{A}	vector column of upper-node voltages (V)
acw	anti-clockwise

ALD	atomic layer deposition
A_n	voltage phasor at the n th node of the upper stringer (V)
B	(wavefield) magnetic flux density vector (T)
B	vector column of lower-node voltages (V)
B	magnetic flux density magnitude (T)
\mathbf{B}_0, B_0	externally imposed constant, uniform magnetic flux density (T)
B_n	voltage phasor at the n th node of the lower stringer (V)
C	capacitance (F)
\hat{C}	capacitance matrix per unit length (F m ⁻¹)
CCD	charge-coupled device (CCD camera)
CCP	capacitively coupled plasma
c	contour
c	speed of light in vacuum
c	(subscript) collisional
cw	clockwise
CW	continuous wave; steady state
d	reactor height between a top-plate and a baseplate
d_s	source height above an interface
ds	elemental length vector along a contour
D	connection configuration term
DC	direct current, time-constant value
DLC	diamond-like carbon
e	the base of natural logarithms, Euler's number (2.718...)
e	electron (subscript)
E	(wavefield) electric field intensity vector (V m ⁻¹)
E -mode	coupling via the E field; see CCP
EM	electromagnetic
EM -mode	coupling via EM fields; see EMCP
EMC	electromagnetic compatibility
EMCP	electromagnetically coupled plasma
eq	equivalent circuit value
FTIR	Fourier transform infrared
FWHM	full width at half maximum
f	current feed point (subscript)
f	frequency (Hz)
f_{RF}	RF frequency (Hz)
f_{pe}	electron plasma frequency (Hz)
f_{pi}	ion plasma frequency (Hz)
f_p	plasma frequency (Hz)
G	conductance per unit length (S m ⁻¹)
g	ground point (subscript)
h	height of an antenna above a baseplate
H	magnetic field strength vector (A m ⁻¹)
H	helicon
H -mode	coupling via the H field; see ICP
I	leg current column vector (A)
I	current (A)
ICP	inductively coupled plasma
Im	imaginary part
ISM	International Scientific and Medical standard

I_n	current phasor in the n th leg (A)
i_{line}	current phasor of current along the line (A)
i_{rf}	current phasor of injected RF current (A)
i_0	amplitude of the first harmonic of shell current density (A m^{-1})
i_s	shell current density (A m^{-1})
J_m	first kind of Bessel function, of order m (see Y_m)
J_n	current in the n th upper stringer section (A)
j	$\sqrt{-1}$
K_n	current in the n th lower stringer section (A)
\mathbf{k}	wavenumber vector (m^{-1})
k	magnitude of the wavenumber vector \mathbf{k} (m^{-1})
k_0	wavenumber in vacuum; $k_0 = \omega/c$ (m^{-1})
k_d	wavenumber in a dielectric (m^{-1})
k_z	axial wavenumber, along z (m^{-1})
k_{\perp}	perpendicular wavenumber, perpendicular to z (m^{-1})
k_B	Boltzmann's constant ($1.38 \cdot 10^{-23} \text{ J K}^{-1}$)
LHS	left-hand side
L	self partial inductance (H)
\hat{L}	self partial inductance per unit length (H m^{-1})
L_{leg}	self partial inductance of a leg (H)
L_{str}	self partial inductance of a stringer segment (H)
L^{loop}	loop self inductance of a wire loop, coil, or solenoid (H)
\hat{L}^{loop}	loop self inductance per unit length of a transmission line (H)
L_i^{loop}	contribution to loop self inductance of the i th wire segment (H)
l	length of a wire, or an antenna leg
leg	leg (or rung) across the ladder width; or a birdcage leg
MRI	magnetic resonance imaging
\hat{M}	mutual partial inductance matrix per unit length (H m^{-1})
M_{ij}	mutual partial inductance between wire filaments i and j (H)
m	mode number
m	azimuthal periodicity
m_e	electron mass (kg)
mes	measured, or measurement
NMR	nuclear magnetic resonance
N	total number of legs
N	refractive index
nc	(subscript) non-collisional, or collisionless
n_{e0}	time-constant electron number density (m^{-3})
OTR	oxygen transmission rate ($\text{c.c. m}^{-2} \text{ atm}^{-1} \text{ day}^{-1}$)
PEC	perfect electric conductor
PECVD	plasma-enhanced chemical vapour deposition
P_{rf}	RF input power (W)
\hat{P}	Maxwell's potential coefficient matrix (V)
p.u.l.	per unit length (signified by a hat above the symbol)
q	magnitude of the electron charge; $q = +1.602 \cdot 10^{-19} \text{ C}$
Q	quality factor
RAID	Resonant Antenna Ion Device
Re	real part
res	resonance (subscript or superscript)
RF, rf	radio frequency

RHS	right-hand side
R	resistance, real impedance (Ω)
\hat{R}	resistance per unit length (Ω/m)
R, r	radius (m)
r	resistance (Ω)
\mathbf{S}	Poynting's vector $\mathbf{E} \times \mathbf{H}$ (W m^{-2})
S	area (m^2)
S_n^J	source current at the n th node of the upper stringer (A)
S_n^K	source current at the n th node of the lower stringer (A)
sccm	a gas mass flow rate in standard cubic centimetres per second
Scrn	algebraic terms depending on currents induced in a PEC screen
SiO_x	silicon oxide with intermediate stoichiometry; $x = 1\text{--}2$
SLM	a gas mass flow rate in standard litres per second
str	stringer, along the length of a ladder
T	absolute temperature (K)
T_e	electron temperature
T	Trivelpiece–Gould mode (subscript)
T–G	Trivelpiece–Gould mode
TM	transverse magnetic
\tilde{U}_L	lower shift matrix
V_{pp}	peak-to-peak voltage (V)
V_{rf}	phasor of the applied RF voltage (V)
v	velocity (m s^{-1})
v	phase velocity (m s^{-1})
W -mode	coupling via helicon wave fields
\tilde{X}	$N \times N$ matrix for parameters X_{nm}
\mathbf{X}	column vector array for parameters X_n
X	reactive (imaginary) impedance (Ω)
$\hat{\mathbf{x}}$	unit vector along the x -axis
Y	complex admittance (S)
Y_{eq}	complex equivalent circuit admittance at resonance (S)
$\hat{\mathbf{y}}$	unit vector along the y -axis
Y_m	second kind of Bessel function, of order m (see J_m)
Z	complex impedance (Ω)
Z_{str}	stringer complex impedance (Ω)
Z_{leg}	leg complex impedance (Ω)
Z_c	characteristic impedance of a transmission line (Ω)
$Z_{\text{in}}^{\text{eq}}$	equivalent circuit complex input impedance (Ω)
$Z_{\text{in}}^{\text{res}}$	complex input impedance at resonance (Ω)
$\hat{\mathbf{z}}$	unit vector along the z -axis